Journal of Membrane Science 660 (2022) 120847

Contents lists available at ScienceDirect

Journal of Membrane Science

journal homepage: www.elsevier.com/locate/memsci

# New sustainable routes for gas separation membranes: The properties of poly(hydroxybutyrate-*co*-hydroxyvalerate) cast from green solvents

Kseniya Papchenko [b], Micaela Degli Esposti [a,b], Matteo Minelli [a,b], Paola Fabbri [a,b], Davide Morselli [a,b,**], Maria Grazia De Angelis [a,b,c,*]

[a] Department of Civil, Chemical, Environmental, and Materials Engineering, DICAM, University of Bologna, Via Terracini 28, 40131, Bologna, Italy
[b] National Interuniversity Consortium of Materials Science and Technology (INSTM), Via Giusti 9, 50121, Firenze, Italy
[c] Institute for Materials and Processes, School of Engineering, University of Edinburgh, Sanderson Building, Robert Stevenson Road, EH9 3FB, UK

A B S T R A C T

The gas separation performance of biopolymers is still scarcely characterized, mostly because of their poor thermomechanical properties and high crystallinity which is associated to low permeability. In this work we characterize the gas transport in a poly(hydroxybutyrate-*co*-hydroxyvalerate) (PHBV) random copolymer, that has a relatively low crystallinity and good mechanical properties, combined with a renewable origin, biodegradability and biocompatibility. In the study we also compared several solvents for membrane casting, with different toxicity levels. We found that dimethyl carbonate allows the production of polymer films with transport properties similar to those obtained with the more toxic $CHCl_3$, and it leads also to stable crystallinity of the samples over time. PHBV films show a size-sieving gas separation behaviour, as the permeability decreases significantly with the gas kinetic diameter. However, the strong energetic interactions of $CO_2$ with the polymer matrix, confirmed by the Flory-Huggins model, induce a marked solubility-driven $CO_2/N_2$ and $CO_2/CH_4$ selectivity, which could make the material potentially interesting for $CO_2$ removal processes.

## Author statement

Kseniya PAPCHENKO: Data curation, Investigation, Writing–original draft; Micaela DEGLI ESPOSTI: Data curation, Writing–review & editing; Matteo MINELLI: Methodology, Supervision, Writing–review & editing; Paola FABBRI: Conceptualization, Supervision; Davide MORSELLI: Conceptualization, Formal Analysis, Writing–review & editing; Maria Grazia DE ANGELIS: Supervision, Conceptualization, Writing–review & editing.

## 1. Introduction

Membrane technology is widely accepted to be a competitive alternative to traditional separation techniques, including the separation of gaseous mixtures, due to its low energy consumption, manufacturing scalability, and reduced footprint [1–5]. Although the overall sustainability of chemical processes can be improved by using membranes, most polymeric membranes and the chemicals used to produce them cannot be considered truly sustainable, since they are fossil-based, and their recyclability is limited, while a full replacement of membrane module is typically required for most industrial applications every three to five years [1,6]. Furthermore, the majority of the polymers traditionally used for gas separation applications require the use of hazardous organic solvents for the membrane manufacturing. The aim of the present work is to evaluate the feasibility of more sustainable alternatives for membrane materials and their fabrication process, such as bio-based and biodegradable polymers [7,8] and green solvents [9,10].

To fulfil the first objective, we explored the membrane potential of a copolymer of the poly(hydroxyalkanoate)s (PHAs) family, linear polyesters produced by bacterial fermentation and known for their fully renewable origin, biodegradability in many environments and physiological biocompatibility [11,12]. The peculiar properties of PHAs, such as hydrophobicity and thermoplastic behaviour, assured the possibility to apply these polymers in different applications, ranging from packaging to the biomedical field [7,13–15]. Poly(3-hydroxybutyrate) (PHB), poly(3-hydroxyvalerate) (P3HV), and their copolymers are currently the most studied and produced bio-polyesters. The gas transport properties of such biopolymers have been partly investigated by

* Corresponding author. Institute for Materials and Processes, School of Engineering, University of Edinburgh, Sanderson Building, Robert Stevenson Road, EH9 3FB, UK.
** Corresponding author. Department of Civil, Chemical Environmental and Materials Engineering, DICAM, University of Bologna, Via Terracini 28, 40131, Bologna, Italy.
*E-mail addresses:* k.papchenko@sms.ed.ac.uk (K. Papchenko), davide.morselli6@unibo.it (D. Morselli), grazia.deangelis@ed.ac.uk (M.G. De Angelis).

https://doi.org/10.1016/j.memsci.2022.120847
Received 25 May 2022; Received in revised form 9 July 2022; Accepted 16 July 2022
Available online 21 July 2022

different groups, revealing promising separation capability, mainly for $CO_2/O_2$ and $CO_2/N_2$ gas pairs [16–19]. In particular, Follain et al. [16] reported selectivities between 1.5 and 6.7 for $CO_2/O_2$ and between 4.8 and 19 for $CO_2/N_2$ for PHB and poly(3-hydroxybutyrate-*co*-3-hydroxyvalerate) (PHBV, 3 mol% 3-HV units), generally higher but still comparable to those reported by Siracusa et al. [17] for PHB. Additionally, Huh et al. [19] reported $H_2$ permeability and selectivity values in PHBV (12 mol% 3-HV units) and composite membranes formed by adding multiwall carbon nanotubes to the polymer. However, the gas permeability and selectivity values reported in that work for pure PHBV seem not consistent with previous ones. In general, the data reported in literature until now are limited by the number of gases investigated, as for instance no data are available for $CH_4$ transport in PHBV.

However, PHB is a highly crystalline and brittle material, and its use as membrane would require additives, plasticizers, or blending with other polymers, such as poly(lactic acid) (PLA) or cellulose [13,20,21]. To control both ductility and crystallinity of PHB it is also possible to introduce 3-hydroxyvalerate (HV) units in its chains and thus obtain the copolymer poly(3-hydroxybutyrate-*co*-3-hydroxyvalerate) (PHBV), which is typically preferred for production of thin films [22]. For this reason, we chose in this work to use a PHBV containing 25 mol% of 3-hydroxyvalerate units, in order to have a more suitable material for membrane-related applications and to extend the knowledge on gas transport properties in this family of polymers.

Typically, membranes are fabricated by means of different methods, all requiring the use of conventional petroleum-derived solvents. Such solvents present both health and environmental hazards, thus a need for greener and less toxic solvents is of great importance [9,23]. An alternative solvent for a specific membrane fabrication should be chosen based on its ability to dissolve the selected polymer and its volatility, which needs to be similar or comparable to the traditional solvent, whereas its reduced adverse effects on health and environment are an essential requirement [9]. From this perspective, five different solvents were selected to fabricate PHBV-based membranes by solvent casting. First, two traditional solvents, chloroform ($CHCl_3$) and dimethylformamide (DMF), were considered in order to obtain membranes suitable for comparison. Dimethyl carbonate (DMC) was selected as a green solvent, given its low (eco)toxicity, low hazard associated with handling, and complete biodegradability [10,24]. The use of two benign and potentially biomass-derived organic acids as acetic ($CH_3COOH$) and formic acid (HCOOH) was also explored [25–28]. The solvent casting protocol was optimized for each solvent, in order to produce self-standing membranes, suitable for further characterization.

The thermal properties of PHBV-based membranes were investigated by differential scanning calorimetry (DSC), whereas their morphology and physical properties were evaluated by scanning electron microscopy (SEM), Fourier transform infrared spectroscopy (FT-IR), and gel permeation chromatography (GPC). Ultimately, the gas transport properties at 35°C were analysed by permeation of He, $N_2$, $CO_2$, $CH_4$ and $O_2$, as well as $CO_2$ sorption tests up to 30 bar.

An analysis of physical, morphological, and transport properties and their dependence on solvent used in the casting protocol was carried out, suggesting a route to obtain bio-based membranes with tuneable features for gas separation applications.

## 2. Experimental

### 2.1. Materials

Bacterial poly(3-hydroxybutyrate) (PHB) and poly(3-hydroxybutyrate-*co*-3-hydroxyvalerate) (PHBV, 25 mol% 3-HV units), were supplied by Sigma-Aldrich as custom grade powder and purified prior to membranes fabrication as described elsewhere [15]. The structure of both polymers is shown in Fig. 1.

Solvents used for membrane preparation, namely chloroform, DMC, DMF, formic acid, acetic acid, together with methanol used for purification, were purchased from Sigma-Aldrich with purities ≥99% and used as received. Gases used for permeation and sorption tests, helium (He), oxygen ($O_2$), nitrogen ($N_2$), methane ($CH_4$), and carbon dioxide ($CO_2$), were purchased from Fluido Tecnica (Campi Bisenzio, FI, Italy) with purities ≥99.5%.

### 2.2. Membrane preparation

PHB and PHBV membranes were prepared through the solvent casting method. The amounts of polymer and solvent needed to reach the desired concentration (Table 1) were mixed and maintained under magnetic stirring for at least 24 h. When the polymer was completely solubilized, the solution was poured onto a Petri dish and left to evaporate at a specific temperature, covered with an aluminium foil. The morphology optimization of the prepared membranes included the analysis of the optimal polymer concentration in each solvent. Such analysis showed that PHB can reach very high concentration in $CHCl_3$, while for PHBV the highest concentration is reached with DMF and the lowest one with DMC, as summarized in Table 1. The thickness of all the obtained membranes ranged between 70 and 100 μm. Each membrane was maintained under dynamic vacuum at room temperature for at least 24 h prior to testing, in order to ensure the complete removal of any residual solvent and atmospheric moisture. The attempts to prepare self-standing homogeneous PHB-based membranes with solvents different from $CHCl_3$ were not successful.

**Table 1**
Membrane preparation protocol parameters.

| Membrane (Polymer-Solvent) | Petri Dish Diameter [mm] | Polymer Concentration [mg $mL^{-1}$] | Evaporation Temperature [°C] | Solvent Boiling Point [°C] |
|---|---|---|---|---|
| PHB-$CHCl_3$ | 50 | 45.5 | Room T | 61 |
| | 70 | 75 | Room T | 61 |
| PHBV-$CHCl_3$ | 70 | 30 | Room T | 61 |
| PHBV-DMF | 50 | 50 | 110 | 153 |
| PHBV-DMC | 70 | 23.1 | 80 | 90 |
| PHBV-HCOOH | 50 | 37.5 | 80 | 101 |
| PHBV-$CH_3COOH$ | 50 | 37.5 | 80 | 118 |

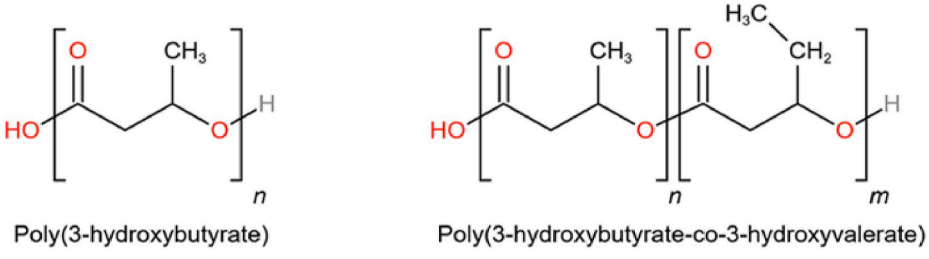


**Fig. 1.** Chemical structures of the biopolyesters used in this study.

### 2.3. Membrane characterization

#### 2.3.1. Gel permeation chromatography (GPC)

Molecular weights of PHBV before and after membrane casting were determined by gel permeation chromatography with an Agilent 1260 Infinity instrument (G1322A 1260 Degasser, G1310B 1260 Isocratic Pump, G1316A 1260 TCC thermostatted Column Compartment, G1362A 126 RID Reflective Index Detector, G1328C 126 Manual Injector), in order to investigate potential polymer degradation due to the solvent. RID and column compartment were thermostatically controlled at 35°C ± 0.2°C. The instrument was equipped with a PLgel MiniMIX-A column (20 μm particle size, 4.6 × 250 mm) coupled with a Tosoh TSKgel SuperMultipore HZM column (4 μm particle size, 4.6 × 150 mm). Columns were preceded by a low dispersion in-line filter (frit porosity 0.2 μm). $CHCl_3$ was used as mobile phase at a flow rate of 0.2 mL $min^{-1}$ and toluene was used as internal standard (0.1 μL $mL^{-1}$), with a run time of 37 min. Data were processed with Agilent GPC/SEC software, version A.02.01 using a calibration curve obtained with monodispersed polystyrene standards (EasiCal PS-1 Agilent kit).

#### 2.3.2. Scanning electron microscopy (SEM)

Membranes morphology was investigated using a scanning electron microscope Nova NanoSEM (FEI), applying 15 KeV. The cross-sections were prepared by fracturing the specimens in liquid nitrogen and placing them on a stub by using a carbon tape; the electrical conductivity was guaranteed through a silver paste line. Before the SEM investigation, the specimens were coated with approx. 10 nm of gold. The analysis of SEM images was carried out using FIJI/ImageJ open-source software.

#### 2.3.3. Differential scanning calorimetry (DSC)

Thermal properties of the prepared materials were evaluated by differential scanning calorimetry (Q10, TA Instruments), fitted with a standard DSC cell, and equipped with a Discovery Refrigerated Cooling System (RCS90, TA Instruments). Measurements were performed under dry nitrogen flow (50 mL $min^{-1}$) on samples of approximately 10 mg, placed in an aluminium pan. The samples were analysed applying thermal cycle from −60°C to 195°C (hold for 2 min) with a heating rate of 10°C $min^{-1}$ and a cooling rate of 20°C $min^{-1}$. DSC curves were analysed by TA Universal Analysis 2000 to determine the glass transition temperature ($T_g$). The degree of crystallinity ($X_c$) was calculated as follows:

$$X_c = \Delta\widehat{H}_m / \Delta\widehat{H}_m^0 \tag{1}$$

where $\Delta\widehat{H}_m$ is the melting enthalpy calculated from the endothermic peak recorded during the heating, while $\Delta\widehat{H}_m^0$ is the heat of melting of purely crystalline PHB, equal to 146 J $g^{-1}$ [16,29]. This value is typically used for PHBV with less than 40 mol% 3-HV units, which are partially excluded from PHB crystalline lattice [30].

#### 2.3.4. Fourier-transform infrared spectroscopy (FT-IR)

The chemical structure of the membranes was analysed through FT-IR (PerkinElmer Spectrum Two), in attenuated total reflectance (ATR) mode, from 4000 to 400 $cm^{-1}$. The resolution was set to 4 $cm^{-1}$, and 64 scans were collected for each spectrum. Moreover, the absence of residual solvent and/or humidity was determined using the same procedure. FT-IR spectra were analysed by Spectrum 10, in order to obtain absorbance of relevant peaks of the material. All samples were tested after a vacuum treatment.

#### 2.3.5. Permeability measurements

Pure gas permeability of He, $N_2$, $O_2$, and $CO_2$ was measured at 35°C for purified PHBV membranes prepared by $CHCl_3$, while permeability of He, $N_2$, $CH_4$, and $CO_2$ was evaluated at the same temperature for the membranes prepared with DMC. The fixed-volume variable-pressure manometric technique used and the equipment set-up were schematically represented and described elsewhere [31,32]. Each permeability experiment was performed at an absolute upstream pressure of about 1.3 bar and initial vacuum condition on the permeate membrane side.

Permeability of the component $i$, $P_i$, is proportional to the molar flux $J_i$, as described in **Section S1.1**, and measures the ability of the membrane material to permeate gas. Assuming the validity of the Fick's law to describe the diffusion in the membrane, and assuming the phase equilibrium at the gas-membrane interface, the solution-diffusion model is obeyed [33] and the permeability coefficient can be split into two factors: the diffusion coefficient, $\mathscr{D}_i$, and the solubility coefficient, $S_i$:

$$P_i = \mathscr{D}_i S_i \tag{2}$$

The diffusion coefficient is a predominantly kinetic factor that measures the mobility of different species in the polymeric matrix, while the solubility coefficient reflects the sorption capacity of the polymer towards different species and it is thermodynamically driven. Gas diffusivity is evaluated by means of the time-lag method, as discussed in **Section S1.1**.

The ratio between pure gas permeabilities provides an indication of the ability of the membrane to separate two gases. Such parameter is called the ideal selectivity, and under the assumption of solution-diffusion model and negligible downstream pressure, it can be conveniently split into diffusivity selectivity, $\alpha_{ij}^{\mathscr{D}}$, and solubility selectivity, $\alpha_{ij}^{S}$, as follows:

$$\alpha_{ij} = \frac{P_i}{P_j} = \frac{\mathscr{D}_i S_i}{\mathscr{D}_j S_j} = \alpha_{ij}^{\mathscr{D}} \alpha_{ij}^{S} \tag{3}$$

If the solution-diffusion model holds true, one can estimate the solubility from the results of a permeation experiment where both permeability and diffusivity are obtained and compare it to solubility coefficients obtained from direct sorption experiments.

Noticeably, in most semicrystalline materials, such as in our case, the crystal domains are practically impermeable to penetrating gases, in view of their larger density, and are thus not involved in gas sorption and diffusion processes, which occur only in the surrounding amorphous phase. The presence of impermeable crystallites, however, affects both solubility and diffusivity of the resulting semicrystalline material. A thorough analysis of such effects was beyond the purpose of this paper, but we address the reader to specific works focused on such issue [34]. Noteworthy, the properties obtained from permeation and sorption tests and presented in this manuscript, namely permeability, diffusivity and solubility coefficients, are referred to the semicrystalline material, and thus depend on the amount and morphology of the crystalline domains of the sample, unless otherwise specified.

#### 2.3.6. Solubility measurements

Solubility and diffusivity of $CO_2$ in PHBV-$CHCl_3$ membrane were also determined at 35°C in a wide pressure range (up to 30 bar) by direct sorption in a pressure decay apparatus. The density of the semicrystalline membrane was calculated as equal to 1.204 g $cm^{-3}$, based on crystal and amorphous densities, reported by Mitomo et al. for a 25% 3-HV copolymer [35], and crystallinity degree measured one month after casting. The thickness of the membrane was measured to be 105 ± 7 μm. In the pressure decay technique, a known amount of gas is fed into the sample chamber and the mass uptake is evaluated by measuring the pressure decrease of the mass uptake till the constant value is reached. Subsequent sorption tests are performed by increasing the external pressure in a stepwise manner, to obtain the sorption isotherm in the pressure range of interest. In the present study, the pressure was monitored by two manometers (Sensotec Super TJE), the first one having a full scale of 14 atm, the second one of 34 atm. Both manometers have an accuracy equal to 0.05% of the full-scale value and they can be connected to the experimental chamber in different pressure intervals

within the same isothermal experiment, in order to maintain a good level of sensitivity at any pressure. The full equipment set-up is well represented and described elsewhere [36]. The penetrant diffusivity in the film can be evaluated from the sorption kinetics, by considering Fickian diffusion and the variation of interfacial concentration during the experiment, as reported in **Section S1.2**.

## 3. Results and discussion

The PHB and PHBV-based membranes were prepared through solvent casting technique, with a protocol optimized for each solvent, as reported in Table 1. As shown by Fig. 2, the PHB membrane is less transparent if compared with the PHBV-based membranes. In addition, the membranes fabricated using PHBV are generally more flexible than those based on PHB, while their grade of transparency depends on the casting protocol. In particular, the use of DMC and HCOOH leads to membranes with the most homogeneous aspect.

Numeral average molecular weight ($M_n$), weight average molecular weight ($M_w$) and polydispersity index (PDI, as $M_w/M_n$) determined by GPC, are reported in Fig. 3a for all the investigated PHBV-based membranes.

The analysis of $M_w$ distribution of the PHBV membranes with respect to the purified material (purification procedure reported in experimental section) indicates that the solvent-casting method partially affects the polymer. Indeed, samples processed with DMF, acetic and formic acids show a significant $M_w$ decrease with respect to the undissolved polymer. When an acidic solvent is used, like formic and acetic acid, the acid-catalysed hydrolysis of the ester groups can take place, thus breaking the polymeric chains down and lowering both $M_n$ and $M_w$ (Fig. 3a) [37]. In the case of a non-protic solvent as DMF, which presents the highest boiling point among the tested solvents (Table 1) samples were treated at high temperature (110°C). Such aspect may explain the fact that this sample has a low $M_w$, which can be due to a partial degradation due to the combined effect of temperature and solvent [38].

On the contrary, the use of solvents as $CHCl_3$ and DMC does not induce significant change in the polymer $M_w$ values and PDIs, which are equal to those of the as purified material. More in detail, the PDI remains approximately constant (between 3.1 and 3.4) regardless of the solvent used. Such small variations are a well-known aspect of the so-called bacterial polymers (such as PHAs), and are typically accepted [15].

Mechanical properties, such as tensile stress and Young's modulus, are also known to be affected by the molecular weight in PHBV [38]. However, the most important variation in such properties takes place for $M_w$ values considerably lower than those observed in this work, thus no significant difference in the mechanical strength of prepared membranes is expected.

The FT-IR spectra of the PHBV membranes are depicted in Fig. 3b. The spectrum of the PHB membrane is also reported and used for comparison sake. The results confirm the absence of residual solvent and humidity in all samples, as no relevant peaks can be observed in the range between 4000 and 3000 $cm^{-1}$. Despite the aforementioned changes in $M_w$, the solvent casting procedure does not modify the PHBV chemical structure, as the spectrum of PHBV membranes does not change when different solvents are used. Some minor differences can be observed in the spectra of PHBV and PHB (Fig. 3b), essentially associated to the higher crystallinity observed in PHB (value of 62%) with respect to the one observed in the PHBV samples (about 40%). In particular, the peak at 2881 $cm^{-1}$, visible in Fig. 3c and corresponding to the stretching of the C–H bond, is observed in both PHB and PHBV samples as it is not affected by the crystallinity degree. In the same Figure, the shoulder at 3009 $cm^{-1}$, corresponding to the stretching of the same bond when involved in the C–H···O═C interactions [39,40], is associated to the extent of crystallinity, and indeed it is present in the PHB sample while it tends to decrease or disappear in PHBV ones. Finally, we also analysed the peaks at 1721 and the shoulder at 1738 $cm^{-1}$, in Fig. 3d. In a fully amorphous structure, such peak, located at 1738 $cm^{-1}$ [39,40], is commonly attributed to the vibration of the C═O band present in both the chemical structures of PHB and PHBV. When the crystallinity of the polymer increases, the peak shifts to lower wavenumbers, due to the presence of C–H···O═C interactions that

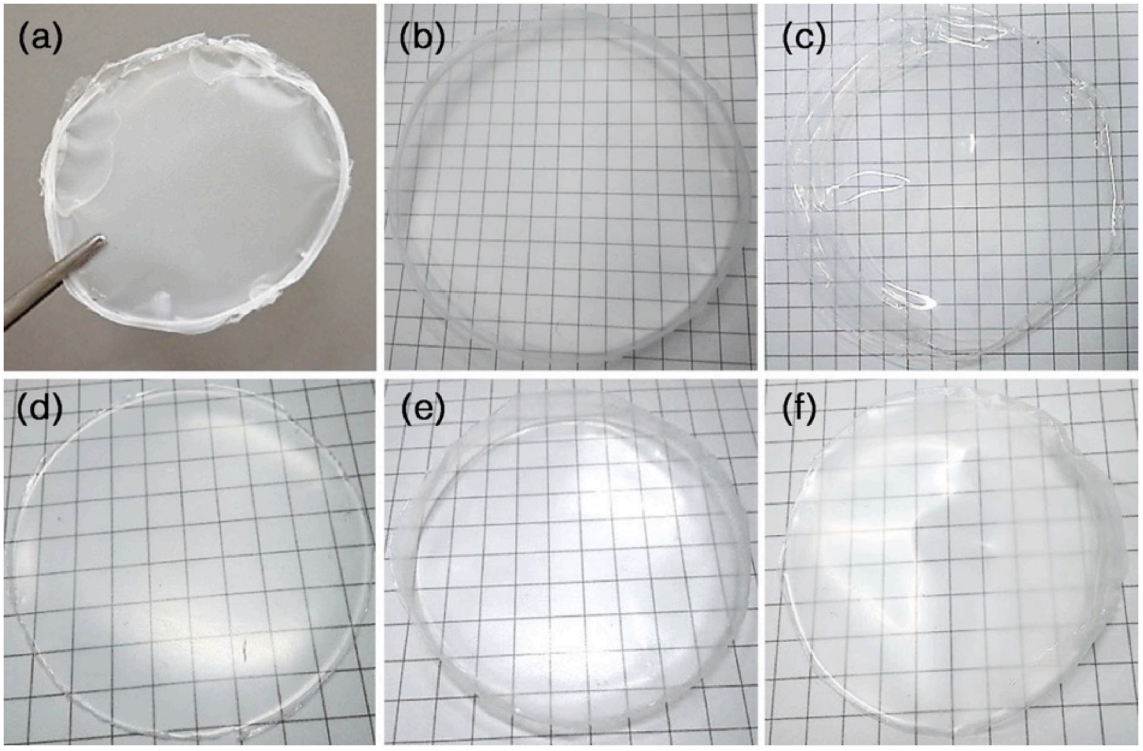


**Fig. 2.** Photographs of (a) PHB film obtained from $CHCl_3$ and PHBV-based membranes prepared by different solvents: (b) $CHCl_3$, (c) DMC, (d) DMF, (e) HCOOH, and (f) $CH_3COOH$.

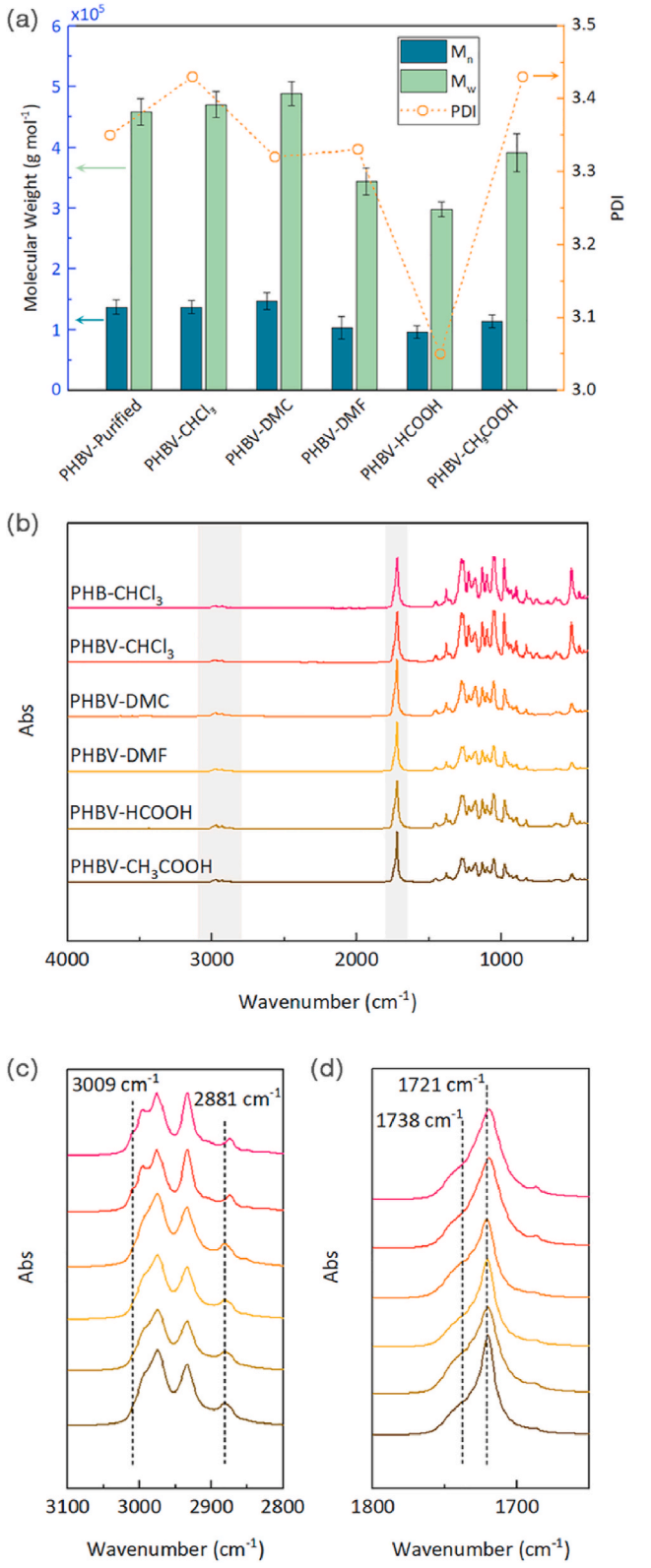


**Fig. 3.** (a) Molecular weight ($M_w$, light green), numeral average molecular weight ($M_n$, dark green) and polydispersity index (PDI, orange line) of purified PHBV and PHBV-based membranes prepared in different solvents. (b) FT-IR spectra of the analysed prepared membranes. (c) Signals associated to C–H bond stretching in PHB- and PHBV-based membranes. (d) Signals correspondent to C═O band vibration in PHB- and PHBV-based membranes. (For interpretation of the references to colour in this figure legend, the reader is referred to the Web version of this article.)

stabilize the typical PHB α-form unit cell in the crystalline phase [40,41]. Therefore, in the semicrystalline PHB and PHBV samples we observed both these two features, as reasonable. However, when calculating the ratio of the absorbance of the crystalline phase (peak at 1721 $cm^{-1}$) to the sum of that of the two phases (crystalline and amorphous), we get different values: 0.72 for PHB-$CHCl_3$ membrane and 0.67 value for PHBV-$CHCl_3$ membrane, highlighting the lower crystallinity of this latter sample that was also measured via other tests.

The cross-section morphology of the prepared membranes was analysed by SEM. Fig. S2 presents the cross-section of PHBV membranes prepared with $CHCl_3$ and DMC, as representative. Both membranes are fully dense and homogeneous without any voids/porosity that could affect the gas transport properties.

The thermal properties and crystallinity degree of the prepared membranes were evaluated through DSC measurements. One example of DSC scan was reported in Fig. S3 in the Supplementary Information for the PHB-$CHCl_3$ sample. We have estimated the crystallinity values to be affected by a 2% error based on the calculation procedure which requires drawing a baseline to estimate the peak area as reported in Fig. S3. All the specimens were tested one and three months after casting, to evaluate the influence of the casting protocol on the secondary crystallization, which typically takes place in PHAs even at room temperatures [12,42]. The PHBV-$CHCl_3$ and PHBV-DMC crystallinities were also measured after eight months, as these membranes showed the most stable behaviour. The results are summarized in Table 2. In particular, membranes prepared from DMF, formic and acetic acid show higher crystallinity with respect to chloroform and DMC-based membranes. Interestingly, the PHBV-DMF membrane exhibits the highest crystallinity degree, 0.47, thanks to a significant increase over time (+37% as crystalline variation) after three months from membrane formation. Furthermore, the $T_g$ increases accordingly with the elapsed time for all samples. Such effect is likely associated to an increase of the size of the rigid crystalline domains, which constrain the chain mobility of the amorphous portion of the polymer.

Considering the GPC results, the crystallinity degree variation on different samples can be attributed to their chains mobility, which leads to a quicker crystallization for the polymers with lowest $M_w$ after the interaction with the solvent. The relationship between the crystallinity degree and time is reported in Fig. 4a. Interestingly, the experimental data show a square root time dependence, as follows:

$$X_c = X_{p,\infty}\left(1 + k_s t^{1/2}\right) \tag{4}$$

where $k_s$ is the rate of crystallinity variation, attributed to secondary crystallization, while $X_{p,\infty}$ is the crystallinity of the sample at the end of the primary crystallization process [43,44]. It can be clearly observed that membranes prepared with $CHCl_3$ and DMC present the lowest crystallinity variation with time, while the samples prepared with formic and acetic acid behave similarly, with variation rate intermediate to those of DMF and DMC/$CHCl_3$-based membranes. An uncertainty of 2% on the crystallinity degree leads to errors as large as 50% in the determination of $k_s$, thus the following discussion carries a qualitative character, useful to understand the general behaviour of the inspected membranes.

The linear dependency of $k_s$ on molecular weight in different samples is shown in Fig. 4b. As expected, higher molecular weight chains have a reduced mobility that leads to low crystallization rate, which results in a higher stability to secondary crystallization. The behaviour of the DMF-based membrane is significantly far from the best-fit line, presenting much higher rate of crystallinity variation with respect to its molecular weight. A similar behaviour was observed on syndiotactic poly(styrene), showing that the crystallinity rate can increase when the PDI decreases due to higher mobility of the macromolecular chains [45].

The analysis of polymer crystallinity, its behaviour over time and its correlation with polymer structural features allows to tailor the membrane properties based on the desired outcome. In particular, since the

**Table 2**
*Glass transition temperature ($T_g$), crystallinity degree ($X_c$) and crystallinity variation ($\Delta X_c$) of the analysed membranes at different times.*

| | PHBV- $CHCl_3$ | | | PHBV- DMC | | | PHBV- DMF | | PHBV- $CH_3COOH$ | | PHBV- HCOOH | |
|---|---|---|---|---|---|---|---|---|---|---|---|---|
| Time [months] | 1 | 3 | 8 | 1 | 3 | 8 | 1 | 3 | 1 | 3 | 1 | 3 |
| $T_g$ [°C] | −12 | −4.9 | −1.8 | – | −6.4 | −5.0 | −5.9 | −4.3 | −13 | −4.9 | −8.1 | −5.3 |
| $X_c$ | 0.39 | 0.42 | 0.43 | 0.38 | 0.41 | 0.42 | 0.35 | 0.47 | 0.40 | 0.45 | 0.37 | 0.44 |
| $\Delta X_c$ [%] | | +7.69 | +10.3 | | +7.89 | +10.3 | | +36.6 | | +11.6 | | +17.8 |

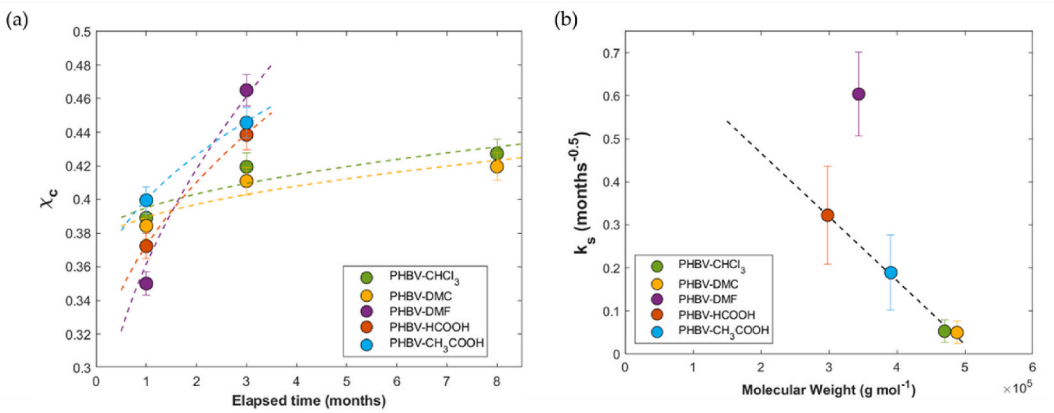


**Fig. 4.** (a) Degree of crystallinity ($X_c$) of PHBV-based membranes as function of the elapsed time; (b) Crystallization rate ($k_s$) of PHBV-based membranes as function of Molecular weight ($M_w$). In (a) the dashed lines are the best fit of Equation (4); in (b) the line is the best linear fit for all membranes, except PHBV-DMF.

transport properties of the polymers are strongly affected by the crystallinity, the $CHCl_3$ and DMC-based membranes were selected for further analysis, as they showed the most stable crystalline value.

### 3.1. Transport properties analysis

The PHBV-based membranes, prepared by solvent casting using either $CHCl_3$ or DMC, were selected for analysing the transport behaviour. The PHB-based samples resulted to be very brittle, and thus the formation of cracks when the membrane is placed into the permeation cell prevented any possibility to test such specimens for gas permeability.

The choice of PHBV-$CHCl_3$ and PHBV-DMC is quite straightforward considering the results of physical and chemical analyses. In fact, the selected membranes showed less degradation due to solvent interaction, good morphological properties and the lowest secondary crystallization rate, thus the highest structural stability.

### 3.2. Permeation

Pure gas permeability of He, $N_2$, $O_2$, $CH_4$, and $CO_2$ was measured at 35°C in PHBV membranes. In order to evaluate the effect of the solvent on the gas transport properties of the PHBV membranes, the tests were carried out for the permeability of He, $N_2$, and $CO_2$ on membranes casted from both $CHCl_3$ and DMC solutions. Since the gas permeability values resulted very similar for the two membranes (difference in the order of less than 30%, except for $N_2$), we concluded that permeability values are independent on the used solvent. Such result is particularly important because it implies that chloroform can be replaced by a greener solvent, according to the safety, health and environmental criteria, namely DMC [24] without affecting the overall properties, as demonstrated above, and the permeability.

The values of permeability and diffusivity are obtained directly from permeation tests, while the solubility coefficients are calculated as the ratio between the two, relying on the solution-diffusion model [33]. However, gas solubility and diffusivity were also evaluated directly by sorption tests, analysed in the following section, and the results obtained for $CO_2$ will be compared with those estimated indirectly by permeation tests.

The results of gas permeation in PHBV membranes are in Table 3 in terms of permeability, diffusivity and solubility. The results obtained will be then be correlated with the properties of pure gaseous penetrants, in particular with gas molecule dimension through the kinetic diameter, and with the gas condensability through critical temperature. Overall, the values of transport properties are similar in the two membranes, consistently with the similarity in their physical and chemical properties and crystalline degree. The only gas for which the two samples seem to show a different permeability is $N_2$: such gas however is characterized by a very low permeability close to the resolution of our instrument, estimated to be ±0.006 Barrer, and a higher scattering of the data is to be expected.

The permeability values are comparable with other polymers of similar nature and structure, such as other PHAs or PLA [16,17,46]. For the $CO_2/N_2$, $CO_2/CH_4$ and $CO_2/O_2$ cases the ideal separation performance is solubility-driven, because the value of the solubility-selectivity is significantly higher than that of diffusion-selectivity, in some cases even unfavourable to $CO_2$. As a result, the polymer shows promising values of the $CO_2/N_2$ and $CO_2/CH_4$ ideal selectivity: 23 ÷ 46 and 26, respectively.

The membrane shows a size-selective behaviour, where permeability decreases with the gas kinetic diameter. On the permeability vs. kinetic diameter plot (Fig. 5a), the $CO_2$ permeability stands well above the correlating line, thanks to the prevailing favourable contribution of solubility, yielding promising values for the $CO_2/N_2$ and $CO_2/CH_4$ selectivity.

It is possible to analyse separately the diffusion and sorption contributions to permeation. The diffusivity follows the following order: $\mathscr{D}_{He} > \mathscr{D}_{O_2} > \mathscr{D}_{N_2} \approx \mathscr{D}_{CO_2} > \mathscr{D}_{CH_4}$, in which the gas size has the predominating effect, and the diffusion coefficient can be correlated to the gas kinetic diameter $d_k$ through an exponential correlation:

$$\mathscr{D} = A \cdot exp(B \cdot d_k) \tag{5}$$

However, there is the exception of $CO_2$, that has a diffusion coefficient smaller than the one that could be predicted based on its size, as shown in Fig. 5b. Such behaviour was also observed in the case of another biodegradable polyester, PLA, as it will be shown in what

**Table 3**
Permeability (P), Diffusivity (D), Solubility (S), and Selectivity values of PHBV-based membranes.

| | PHBV-$CHCl_3$ | | | PHBV-DMC | | |
|---|---|---|---|---|---|---|
| | P [Barrer] | D × $10^8$ [$cm^2$ $s^{-1}$] | S [$cm^3$(STP)/($cm^3$ bar)] | P [Barrer] | D × $10^8$ [$cm^2$ $s^{-1}$] | S [$cm^3$(STP)/($cm^3$ bar)] |
| He | 1.5 ± 0.4 | 87 ± 17 | 0.013 ± 0.003 | 2.0 ± 0.4 | 110 ± 20 | 0.014 ± 0.004 |
| $CO_2$ | 0.7 ± 0.1 | 0.36 ± 0.07 | 1.5 ± 0.4 | 0.5 ± 0.1 | 0.32 ± 0.06 | 1.25 ± 0.31 |
| $O_2$ | 0.11 ± 0.04 | 2.0 ± 0.4 | 0.04 ± 0.01 | – | – | – |
| $N_2$ | 0.03 ± 0.01 | 0.45 ± 0.09 | 0.04 ± 0.01 | 0.01 ± 0.006 | 0.24 ± 0.05 | 0.04 ± 0.01 |
| $CH_4$ | – | – | – | 0.02 ± 0.01 | 0.17 ± 0.03 | 0.09 ± 0.02 |
| | $\alpha_P = P_i/P_j$ | $\alpha_D = D_i/D_j$ | $\alpha_S = S_i/S_j$ | $\alpha_P = P_i/P_j$ | $\alpha_D = D_i/D_j$ | $\alpha_S = S_i/S_j$ |
| $He/CO_2$ | 2.2 ± 0.1 | 240 ± 20 | 0.009 ± 0.001 | 4.0 ± 0.3 | 340 ± 30 | 0.011 ± 0.002 |
| $He/N_2$ | 51 ± 11 | 193 ± 16 | 0.33 ± 0.04 | 185 ± 65 | 450 ± 45 | 0.35 ± 0.05 |
| $CO_2/N_2$ | 23 ± 4 | 0.80 ± 0.07 | 38 ± 5 | 46 ± 17 | 1.3 ± 0.1 | 31 ± 4 |
| $CO_2/O_2$ | 6.3 ± 1.3 | 0.18 ± 0.02 | 36.1 ± 4.6 | – | – | – |
| $CO_2/CH_4$ | – | – | – | 26 ± 12 | 1.9 ± 0.1 | 13.9 ± 1.5 |

follows [46]. Therefore, the correlation coefficient obtainable when considering $CO_2$ in Equation (6) is lower than the one calculated when $CO_2$ diffusivity is not included, the latter reported in Table 4.

The solubility coefficient, estimated as the ratio between permeability and diffusivity, decreases in the following order: $S_{CO_2} > S_{CH_4} > S_{O_2} \approx S_{N_2} > S_{He}$, which is opposite to the diffusivity one. Indeed, as far as solubility is concerned, the condensability of the gas is the most important parameter, which can be expressed by its critical temperature and is generally an increasing function of the gas size. According to this approach, one can draw an exponential correlation between the solubility coefficient and the critical temperature $T_{c,}$ just as it was done for diffusivity. However most often such a relationship is rather expressed as follows:

$$Ln(S) = C \cdot T_c + E \tag{6}$$

It can be noticed in Fig. 5c that the solubility of $CO_2$ is higher than what would be predicted based on its condensability only, due to strong energetic interactions between such penetrant and the polymer matrix with respect to the other gases.

The values of parameters A, B, C, and E, as well as correlation coefficients, are reported in Table 4.

### 3.3. Sorption

To further investigate the interactions of $CO_2$ with the polymer matrix evidenced by the permeability analysis, we measured the sorption isotherm of $CO_2$ in PHBV-$CHCl_3$ membrane at 35°C up to 30 bar: two subsequent runs were performed and the results are shown in Fig. 6a. In Fig. 6a, we also reported previously published data on a PHBV (24 mol% of 3-HV units) membrane casted from $CHCl_3$ solution [22], for which the sorption isotherm lies slightly below the ones measured in this work. The $CO_2$ solubility value calculated from permeability and diffusivity data is also reported, and its value lies close to the measured one, with a positive deviation of 43%. The data were compared to the prediction of the Flory-Huggins (FH) model, which relates the penetrant (1) activity to its concentration in the amorphous polymer (2), expressed in terms of volume fraction $\Phi_1$ [47–49] by the following equation:

$$\ln(a_1) = \ln(1-\Phi_2) + \left(1 - \frac{1}{r}\right)\Phi_2 + \chi_{12}(\Phi_2)^2 \tag{7}$$

In the above equation, $a_1$ is the gas activity, evaluated as the ratio between $CO_2$ pressure and its vapor pressure at the experimental temperature. In this work we are slightly above the critical temperature of $CO_2$, and the vapor pressure has been replaced by the critical pressure, due to the fact that the temperature inspected (35°C) is very close to the critical temperature of $CO_2$ (31°C). In the model, $r$ is the ratio between the molar volume of the polymer and that of the gas, which is infinite in our case. $\chi_{12}$ is the Flory-Huggins energetic binary parameter, that is usually adjusted on experimental data. The solubility calculated with Eq. 8 is relative to the amorphous phase only, and was thus reported in terms of total mass of semicrystalline polymer, to be compared with the experimental solubility data, by assuming that the crystalline phase does not contribute to sorption. As it can be seen from Fig. 6a, the FH model with a value of $\chi_{12} = 0$ allows to represent with satisfactory accuracy the sorption behaviour in the entire pressure range inspected. According to the regular solutions theory of Hildebrand and Scatchard, its value should be close to zero when the solubility parameters of the two substances are similar, i.e. their intermolecular interactions in the pure component state are alike. Thus, based on what observed in the previous section, we can conclude that $CO_2$ shows good chemical affinity and compatibility with this polyester, leading to a promising sorption-enhanced separation behaviour.

The solubility-driven separations are less prone to performance changes induced by morphological variations of the membrane by the penetrants or by physical ageing, being based mostly on the chemical affinity between the gases and the polymer molecules. The solubility-selectivity indeed would not be damaged by a reduction in crystallinity of the sample, as the interactions between gases and polymer would remain the same, and the solubility of all gases will be varied by an equal amount. Therefore, it is possible to think that a modification of the sample that allows to reduce its crystallinity would cause an enhancement of $CO_2$ permeability without damaging the $CO_2/CH_4$ and $CO_2/N_2$ selectivity, as it would happen in the case of a merely diffusivity-driven separation. Such result motivates to continue studying such materials for gas separations, especially for the $CO_2$-related ones, as their performance could be improved if approaches as blending or Mixed Matrix Membranes are considered in the future.

It is worth noticing that the sorption isotherm is slightly concave, indicating a moderate swelling induced by $CO_2$ on the amorphous phase of the polymer. Indeed, it is known that at higher pressures the $CO_2$ can increase chain mobility in rubbery polymers, leading to such an effect.

Such behaviour is also revealed by the behaviour of the diffusion coefficient estimated from the analysis of the sorption transient as a function of the concentration, as reported in Fig. 6b. The diffusivity exhibits an exponential dependence on concentration, which is consistent with swelling induced by the gas in the amorphous part of the polymer. The values obtained in the second test are slightly higher than those obtained in the first test, but still within the experimental uncertainty.

Fig. 6b allows also to directly compare the diffusivity values obtained through sorption and permeation tests. The values obtained from the two types of experiments are very similar, and the deviations are within the experimental error, indicating a good consistency and reproducibility of the reported data.

#### 3.3.1. Comparison with other biopolymers

The gas sorption and transport properties obtained in this work can be compared to the properties of other biodegradable polyesters, such as poly(lactic acid) [46]. Table S1 reports experimental data from permeation tests at 35°C for PHBV and at 30°C for PLA (*L:D* = 98.7:1.3), and

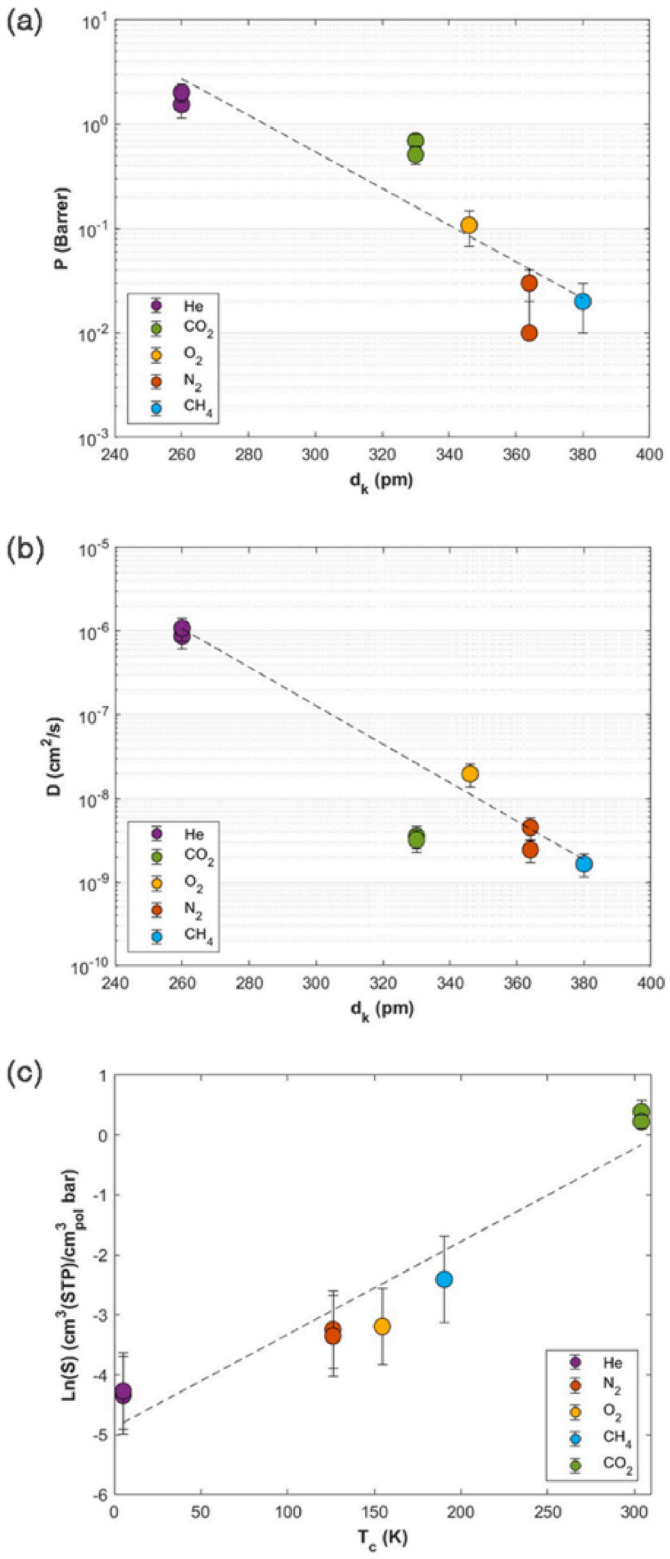


**Fig. 5.** Transport properties of PHBV-$CHCl_3$ and PHBV-DMC membranes with respect to different gases. (a) Permeability and (b) Diffusivity Coefficients are shown as function of kinetic diameter; (c) Solubility Coefficients as function of critical temperature. Fit line in (a) is shown to guide the eye. Fit lines shown in (b) and (c) are referred to data sets without $CO_2$, according to Eqs. (5) and (6).

**Table 4**
Correlation parameters and coefficients for transport properties in PHBV membrane, according to Eqs. (5) and (6).

| Property | Correlation parameters | Without $CO_2$ | $R^2$ |
|---|---|---|---|
| D | A [$cm^2$ $s^{-1}$] | 1.03E+00 | 0.984 |
| | B [$pm^{-1}$] | −5.31E-02 | |
| S | C [$cm^3$(STP)/($cm^3$ bar)] | 9.13E-03 | 0.953 |
| | E [$cm^3$(STP)/($cm^3$ bar K)] | −4.39E+00 | |

summarises such a comparison. Overall, PHBV presents lower permeability and diffusivity values for $CO_2$, $N_2$, and $O_2$, compared to PLA, but higher selectivity. In particular it can be noticed that the permeability of PHBV is about half the value measured in the PLA used as reference, consistently with the fact that such material was practically amorphous (crystallinity lower than 4%), while PHBV has a crystallinity of ~40%.

Thanks to their good energetic interactions with $CO_2$, both PLA and PHBV show a pronounced solubility-selectivity for $CO_2/N_2$ and $CO_2/CH_4$ with a poor diffusivity-selectivity for the same couples. Indeed, the $CO_2$ diffusivity seems to be particularly low in both polymers, especially considering its rather small size: in both cases such aspect can be due to the strong interactions between the gas and the matrix. However, thanks to the high solubility-selectivity for $CO_2$, both membranes have a perm-selectivity favourable to such gas.

Generally speaking, selectivities of PHBV-based membranes result to be in line with those reported for materials already used for $CO_2$ separation, such as cellulose acetate (CA) [50] or Matrimid® [51], while the permeabilities are one order of magnitude lower. Thus, approaches as Mixed Matrix Membranes, where the inclusion of a highly permeable Metal Organic Framework was reported to increase the permeability of pristine matrix by factors as high as 8 [31], can be used in the future to make these polymers competitive for gas separation. Interestingly, this is the first time, to the authors' knowledge, that the permeability of both $CO_2$ and $CH_4$ is reported for a polymer of PHAs family.

## 4. Conclusions

In this work, we studied new green alternatives for membrane separation technology, by evaluating the applicability of a bio-based polymer in typical gas separations, as well as the suitability of green solvents for the membrane fabrication.

The selected co-polyester, PHBV, is a bio-based and biodegradable polymer obtained by bacterial fermentation. Five different solvents, namely $CHCl_3$, DMC, DMF, HCOOH, and $CH_3COOH$, were used in order to produce dense membranes. The solvent nature and evaporation temperature strongly affected the properties of the membranes, specifically their molecular weight and secondary crystallization rate. DMC and $CHCl_3$ are the solvents that allow to obtain the best membrane characterized by the lowest decrease of the $M_w$ due to the procedure and with the lowest second crystallization rate. Samples cast from these solvents were thus characterized in terms of transport properties. It was found that films produced with DMC have transport properties comparable to those obtained with the more toxic $CHCl_3$, which allows to use DMC as a green alternative without compromising the separation performance. The PHBV permeability decreases with the gas kinetic diameter following the order $P_{He} > P_{CO_2} > P_{O_2} > P_{N_2} > P_{CH_4}$. The permeability of $CO_2$ is higher than what would be predicted based on its size, thanks to its high solubility in the polymer, making the PHBV selectivity encouraging for the $CO_2/N_2$ and $CO_2/CH_4$ couples, lying between 26 and 46. The good affinity of $CO_2$ with the polymer was further demonstrated by dedicated sorption tests carried out on this gas, which follows closely the behaviour of regular solutions with a value of the Flory-Huggins parameter equal to zero. Diffusion increases with concentration according to a typical exponential law, due to the swelling experienced by the amorphous portion of the material. The solubility-based separation is particularly promising because it is founded on

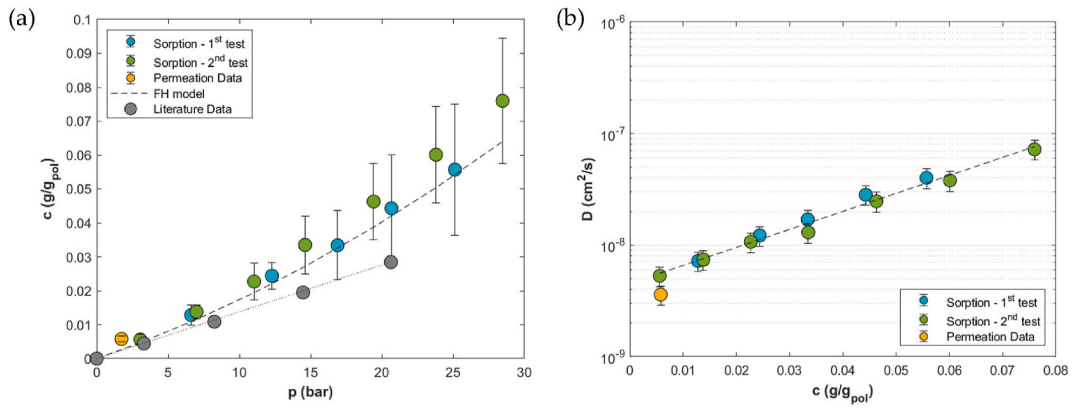


**Fig. 6.** (a) $CO_2$ sorption isotherm in PHBV-$CHCl_3$ membrane at 35°C. The comparison with FH model with $\chi_{12} = 0$ and with literature data is shown [22]. (b) Diffusivity (D) of $CO_2$ as function of average concentration in PHBV-$CHCl_3$, determined from sorption and permeation tests.

energetic interactions rather than on the polymer morphology, in particular its crystallinity. Therefore, a modification that would allow to lower the polymer crystallinity would also enhance the permeability without negatively affecting the selectivity, as it happens with a size-selective material where a free volume enhancement brings an increase of permeability with a simultaneous decrease of selectivity.

In conclusion, the obtained results motivate further explorations into the gas separation abilities of poly (hydroxyalkanoate)s, especially in applications related to $CO_2$ capture.

## Declaration of competing interest

The authors declare that they have no known competing financial interests or personal relationships that could have appeared to influence the work reported in this paper.

## Data availability

Data will be made available on request.

## Appendix A. Supplementary data

Supplementary data to this article can be found online at https://doi.org/10.1016/j.memsci.2022.120847.

## References

[1] R.W. Baker, B.T. Low, Gas separation membrane materials: a perspective, Macromolecules 47 (2014) 6999–7013, https://doi.org/10.1021/ma501488s.
[2] M. Galizia, W.S. Chi, Z.P. Smith, T.C. Merkel, R.W. Baker, B.D. Freeman, *50th anniversary perspective* : polymers and mixed matrix membranes for gas and vapor separation: a review and prospective opportunities, Macromolecules 50 (2017) 7809–7843, https://doi.org/10.1021/acs.macromol.7b01718.
[3] P. Bernardo, E. Drioli, G. Golemme, Membrane gas separation: a review/state of the art, Ind. Eng. Chem. Res. 48 (2009) 4638–4663, https://doi.org/10.1021/ie8019032.
[4] D.F. Sanders, Z.P. Smith, R. Guo, L.M. Robeson, J.E. McGrath, D.R. Paul, B. D. Freeman, Energy-efficient polymeric gas separation membranes for a sustainable future: a review, Polymer 54 (2013) 4729–4761, https://doi.org/10.1016/j.polymer.2013.05.075.
[5] D.S. Sholl, R.P. Lively, Seven chemical separations to change the world, Nature 532 (2016) 435–437, https://doi.org/10.1038/532435a.
[6] G. Owen, M. Bandi, J.A. Howell, S.J. Churchouse, Economic assessment of membrane processes for water and waste water treatment, J. Membr. Sci. 102 (1995) 77–91, https://doi.org/10.1016/0376-7388(94)00261-V.
[7] F. Russo, F. Galiano, A. Iulianelli, A. Basile, A. Figoli, Biopolymers for sustainable membranes in CO2 separation: a review, Fuel Process. Technol. 213 (2021), 106643, https://doi.org/10.1016/j.fuproc.2020.106643.
[8] F. Galiano, K. Briceño, T. Marino, A. Molino, K.V. Christensen, A. Figoli, Advances in biopolymer-based membrane preparation and applications, J. Membr. Sci. 564 (2018) 562–586, https://doi.org/10.1016/j.memsci.2018.07.059.
[9] A. Figoli, T. Marino, S. Simone, E. Di Nicolò, X.-M. Li, T. He, S. Tornaghi, E. Drioli, Towards non-toxic solvents for membrane preparation: a review, Green Chem. 16 (2014) 4034–4059, https://doi.org/10.1039/C4GC00613E.
[10] M.A. Rasool, P.P. Pescarmona, I.F.J. Vankelecom, Applicability of organic carbonates as green solvents for membrane preparation, ACS Sustainable Chem. Eng. 7 (2019) 13774–13785, https://doi.org/10.1021/acssuschemeng.9b01507.
[11] Y. Doi, S. Kitamura, H. Abe, Microbial synthesis and characterization of poly(3-hydroxybutyrate-co-3-hydroxyhexanoate), Macromolecules 28 (1995) 4822–4828, https://doi.org/10.1021/ma00118a007.
[12] K. Sudesh, H. Abe, Y. Doi, Synthesis, structure and properties of polyhydroxyalkanoates: biological polyesters, Prog. Polym. Sci. 25 (2000) 1503–1555, https://doi.org/10.1016/S0079-6700(00)00035-6.
[13] J.Y. Boey, L. Mohamad, Y.S. Khok, G.S. Tay, S. Baidurah, A review of the applications and biodegradation of polyhydroxyalkanoates and poly(lactic acid) and its composites, Polymers 13 (2021) 1544, https://doi.org/10.3390/polym13101544.
[14] M. Vert, Aliphatic polyesters: great degradable polymers that cannot do everything, Biomacromolecules 6 (2005) 538–546, https://doi.org/10.1021/bm0494702.
[15] M. Degli Esposti, F. Chiellini, F. Bondioli, D. Morselli, P. Fabbri, Highly porous PHB-based bioactive scaffolds for bone tissue engineering by in situ synthesis of hydroxyapatite, Mater. Sci. Eng. C 100 (2019) 286–296, https://doi.org/10.1016/j.msec.2019.03.014.
[16] N. Follain, C. Chappey, E. Dargent, F. Chivrac, R. Crétois, S. Marais, Structure and barrier properties of biodegradable polyhydroxyalkanoate films, J. Phys. Chem. C 118 (2014) 6165–6177, https://doi.org/10.1021/jp408150k.
[17] V. Siracusa, C. Ingrao, S.G. Karpova, A.A. Olkhov, A.L. Iordanskii, Gas transport and characterization of poly(3 hydroxybutyrate) films, Eur. Polym. J. 91 (2017) 149–161, https://doi.org/10.1016/j.eurpolymj.2017.03.047.
[18] O. Miguel, M.J. Fernandez-Berridi, J.J. Iruin, Survey on transport properties of liquids, vapors, and gases in biodegradable poly(3-hydroxybutyrate) (PHB), J. Appl. Polym. Sci. 64 (1997) 1849–1859, https://doi.org/10.1002/(SICI)1097-4628(19970531)64:9<1849::AID-APP22>3.0.CO;2-R.
[19] M. Huh, H.M. Lee, Y.S. Park, S.I. Yun, Biocomposite membranes based on poly(3-hydroxybutyrate-co-3-hydroxyvalerate) and multiwall carbon nanotubes for gas separation, Carbon Lett. 21 (2017) 116–121, https://doi.org/10.5714/CL.2017.21.116.
[20] M. Zhang, N.L. Thomas, Blending polylactic acid with polyhydroxybutyrate: the effect on thermal, mechanical, and biodegradation properties, Adv. Polym. Technol. 30 (2011) 67–79, https://doi.org/10.1002/adv.20235.
[21] I.T. Seoane, L.B. Manfredi, V.P. Cyras, Properties and processing relationship of polyhydroxybutyrate and cellulose biocomposites, Procedia Mater. Sci. 8 (2015) 807–813, https://doi.org/10.1016/j.mspro.2015.04.139.
[22] O. Miguel, T.A. Barbari, J.J. Iruin, Carbon dioxide sorption and diffusion in poly(3-hydroxybutyrate) and poly(3-hydroxyvalerate-co-3-hydroxyvalerate), J. Appl. Polym. Sci. 71 (1999) 2391–2399, https://doi.org/10.1002/(SICI)1097-4628(19990404)71:14%3C2391::AID-APP11%3E3.0.CO;2-Q.
[23] X. Dong, D. Lu, T.A.L. Harris, I.C. Escobar, Polymers and solvents used in membrane fabrication: a review focusing on sustainable membrane development, Membranes 11 (2021) 309, https://doi.org/10.3390/membranes11050309.
[24] S.-H. Pyo, J.H. Park, T.-S. Chang, R. Hatti-Kaul, Dimethyl carbonate as a green chemical, Curr. Opinion Green Sust. Chem. 5 (2017) 61–66, https://doi.org/10.1016/j.cogsc.2017.03.012.
[25] P. Anbukarasu, D. Sauvageau, A. Elias, Tuning the properties of polyhydroxybutyrate films using acetic acid via solvent casting, Sci. Rep. 5 (2016), 17884, https://doi.org/10.1038/srep17884.
[26] L. Brunetti, M. Degli Esposti, D. Morselli, A.R. Boccaccini, P. Fabbri, L. Liverani, Poly(hydroxyalkanoate)s meet benign solvents for electrospinning, Mater. Lett. 278 (2020), 128389, https://doi.org/10.1016/j.matlet.2020.128389.
[27] E. Budsberg, R. Morales-Vera, J.T. Crawford, R. Bura, R. Gustafson, Production routes to bio-acetic acid: life cycle assessment, Biotechnol. Biofuels 13 (2020) 154, https://doi.org/10.1186/s13068-020-01784-y.
[28] D.A. Bulushev, J.R.H. Ross, Towards sustainable production of formic acid, ChemSusChem 11 (2018) 821–836, https://doi.org/10.1002/cssc.201702075.

[29] P.J. Barham, A. Keller, E.L. Otun, P.A. Holmes, Crystallization and morphology of a bacterial thermoplastic: poly-3-hydroxybutyrate, J. Mater. Sci. 19 (1984) 2781–2794, https://doi.org/10.1007/BF01026954.
[30] N. Kamiya, M. Sakurai, Y. Inoue, R. Chujo, Isomorphic behavior of random copolymers: thermodynamic analysis of cocrystallization of poly(3-hydroxybutyrate-co-3-hydroxyvalerate), Macromolecules 24 (1991) 3888–3892, https://doi.org/10.1021/ma00013a023.
[31] F.M. Benedetti, M.G.D. Angelis, M.D. Esposti, P. Fabbri, A. Masili, A. Orsini, A. Pettinau, Enhancing the separation performance of glassy PPO with the addition of a molecular sieve (ZIF-8): gas transport at various temperatures, Membranes 11 (2020) 309, https://doi.org/10.3390/membranes11050309.
[32] F02 Committee, Test Method for Determining Gas Permeability Characteristics of Plastic Film and Sheeting, ASTM International, 2010, https://doi.org/10.1520/D1434-82R15E01.
[33] J.G. Wijmans, R.W. Baker, The solution-diffusion model: a review, J. Membr. Sci. 107 (1995) 1–21, https://doi.org/10.1016/0376-7388(95)00102-I.
[34] O. Atiq, E. Ricci, M.G. Baschetti, M.G. De Angelis, Modelling solubility in semi-crystalline polymers: a critical comparative review, Fluid Phase Equil. 556 (2022), 113412, https://doi.org/10.1016/j.fluid.2022.113412.
[35] H. Mitomo, N. Morishita, Structural changes of poly(3-hydroxybutyrate-co-3-hydroxyvalerate) fractionated with acetone-water solution, Polymer 36 (1995) 2573–2578, https://doi.org/10.1016/0032-3861(95)91203-J.
[36] M.C. Ferrari, M. Galizia, M.G. De Angelis, G.C. Sarti, Gas and vapor transport in mixed matrix membranes based on amorphous teflon AF1600 and AF2400 and fumed silica, Ind. Eng. Chem. Res. 49 (2010) 11920–11935, https://doi.org/10.1021/ie100242q.
[37] L.N. Woodard, M.A. Grunlan, Hydrolytic degradation and erosion of polyester biomaterials, ACS Macro Lett. 7 (2018) 976–982, https://doi.org/10.1021/acsmacrolett.8b00424.
[38] S. Luo, D.T. Grubb, A.N. Netravali, The effect of molecular weight on the lamellar structure, thermal and mechanical properties of poly(hydroxybutyrate-co-hydroxyvalerates), Polymer 43 (2002) 4159–4166, https://doi.org/10.1016/S0032-3861(02)00242-2.
[39] H. Sato, Y. Ando, H. Mitomo, Y. Ozaki, Infrared spectroscopy and X-ray diffraction studies of thermal behavior and lamella structures of poly(3-hydroxybutyrate-*co*3-hydroxyvalerate) (P(HB-*co*-HV)) with PHB-type crystal structure and PHV-type crystal structure, Macromolecules 44 (2011) 2829–2837, https://doi.org/10.1021/ma102723n.
[40] H. Sato, Y. Ando, J. Dybal, T. Iwata, I. Noda, Y. Ozaki, Crystal structures, thermal behaviors, and C−H···O═C hydrogen bondings of poly(3-hydroxyvalerate) and poly(3-hydroxybutyrate) studied by infrared spectroscopy and X-ray diffraction, Macromolecules 41 (2008) 4305–4312, https://doi.org/10.1021/ma702222a.
[41] H. Wang, K. Tashiro, Reinvestigation of crystal structure and intermolecular interactions of biodegradable poly(3-hydroxybutyrate) α-form and the prediction of its mechanical property, Macromolecules 49 (2016) 581–594, https://doi.org/10.1021/acs.macromol.5b02310.
[42] M.J. Jenkins, K.E. Robbins, C.A. Kelly, Secondary crystallisation and degradation in P(3HB-co-3HV): an assessment of long-term stability, Polym. J. 50 (2018) 365–373, https://doi.org/10.1038/s41428-017-0012-8.
[43] J.J. Marsh, R.P. Turner, J. Carter, M.J. Jenkins, Thermal diffusivity and secondary crystallisation kinetics in poly(lactic acid), Polymer 179 (2019), 121595, https://doi.org/10.1016/j.polymer.2019.121595.
[44] K. Phillipson, M.J. Jenkins, J.N. Hay, The effect of a secondary process on crystallization kinetics – poly (ϵ-caprolactone) revisited, Eur. Polym. J. 84 (2016) 708–714, https://doi.org/10.1016/j.eurpolymj.2016.09.037.
[45] C.-M. Chen, T.-E. Hsieh, M.-Y. Ju, Effects of polydispersity index and molecular weight on crystallization kinetics of syndiotactic polystyrene (sPS), J. Alloys Compd. 480 (2009) 658–661, https://doi.org/10.1016/j.jallcom.2009.02.003.
[46] L. Bao, J.R. Dorgan, D. Knauss, S. Hait, N.S. Oliveira, I.M. Maruccho, Gas permeation properties of poly(lactic acid) revisited, J. Membr. Sci. 285 (2006) 166–172, https://doi.org/10.1016/j.memsci.2006.08.021.
[47] P.J. Flory, Thermodynamics of high polymer solutions, J. Chem. Phys. 10 (1942) 51, https://doi.org/10.1063/1.1723621.
[48] P.J. Flory, Fifteenth spiers memorial lecture. Thermodynamics of polymer solutions, Discuss. Faraday Soc. 49 (1970) 7, https://doi.org/10.1039/df9704900007.
[49] M.L. Huggins, Solutions of long chain compounds, J. Chem. Phys. 9 (1941) 440, https://doi.org/10.1063/1.1750930, 440.
[50] H. Nguyen, M. Wang, M.-Y. Hsiao, K. Nagai, Y. Ding, H. Lin, Suppression of crystallization in thin films of cellulose diacetate and its effect on CO2/CH4 separation properties, J. Membr. Sci. 586 (2019) 7–14, https://doi.org/10.1016/j.memsci.2019.05.039.
[51] Y. Zhang, I.H. Musselman, J.P. Ferraris, K.J. Balkus, Gas permeability properties of Matrimid® membranes containing the metal-organic framework Cu–BPY–HFS, J. Membr. Sci. 313 (2008) 170–181, https://doi.org/10.1016/j.memsci.2008.01.005.